

## Nanoscale diffraction imaging of the high-pressure transition in Fe<sub>1-x</sub>O

Yang Ding, Zhonghou Cai, Qingyang Hu, Hongwei Sheng, Jun Chang, Russell J. Hemley, and Wendy L. Mao

Citation: [Applied Physics Letters](#) **100**, 041903 (2012); doi: 10.1063/1.3679117

View online: <http://dx.doi.org/10.1063/1.3679117>

View Table of Contents: <http://scitation.aip.org/content/aip/journal/apl/100/4?ver=pdfcov>

Published by the [AIP Publishing](#)

---

### Articles you may be interested in

[Phase transition and huge ferroelectric polarization observed in BiFe<sub>1-x</sub>GaxO<sub>3</sub> thin films](#)

Appl. Phys. Lett. **102**, 222906 (2013); 10.1063/1.4809955

[Polarization fatigue of Pr and Mn co-substituted BiFeO<sub>3</sub> thin films](#)

Appl. Phys. Lett. **99**, 012903 (2011); 10.1063/1.3609246

[Study of Phase Transformations on NanoCrystalline \(La,Sr\)\(Mn,Fe\)O<sub>3</sub> Systems by HighPressure Mössbauer Spectroscopy](#)

AIP Conf. Proc. **845**, 200 (2006); 10.1063/1.2263298

[Zone-axis diffraction study of pressure-induced inhomogeneity in single-crystal Fe 1 - x O](#)

Appl. Phys. Lett. **87**, 041912 (2005); 10.1063/1.1999016

[Variable pressure-temperature neutron diffraction of wüstite \( Fe 1 - x O \) : Absence of long-range magnetic order to 20 GPa](#)

Appl. Phys. Lett. **86**, 052505 (2005); 10.1063/1.1852075

---

An advertisement for Keysight B2980A Series Picoammeters/Electrometers. The text reads: 'Confidently measure down to 0.01 fA and up to 10 PΩ'. Below this is the product name 'Keysight B2980A Series Picoammeters/Electrometers' and a red button that says 'View video demo'. To the right is an image of the device and the Keysight Technologies logo.

## Nanoscale diffraction imaging of the high-pressure transition in $\text{Fe}_{1-x}\text{O}$

Yang Ding,<sup>1,2,a)</sup> Zhonghou Cai,<sup>1</sup> Qingyang Hu,<sup>3</sup> Hongwei Sheng,<sup>3</sup> Jun Chang,<sup>2,4</sup> Russell J. Hemley,<sup>5</sup> and Wendy L. Mao<sup>6</sup>

<sup>1</sup>Advanced Photon Source, Argonne National Laboratory, Argonne, Illinois 60439, USA

<sup>2</sup>HPSynC, Geophysical Laboratory, Carnegie Institution of Washington, 9700 South Cass Ave., Argonne, Illinois 60439, USA

<sup>3</sup>School of Physics, Astronomy and Computational Sciences, George Mason University, Fairfax, Virginia 22030, USA

<sup>4</sup>Department of Physics, Northern Illinois University, DeKalb, Illinois 601155, USA

<sup>5</sup>Geophysical Laboratory, Carnegie Institution of Washington, 5251 Broad Branch Rd., N.W., Washington, DC 20015, USA

<sup>6</sup>Geological and Environmental Sciences, Stanford University, 450 Serra Mall, Stanford, California 94305-2115, USA; Photon Science, and Stanford Institute for Materials and Energy Science, SLAC National Accelerator Laboratory, 2575 Sand Hill Road, Menlo Park, California 94025, USA

(Received 26 November 2011; accepted 3 January 2012; published online 24 January 2012)

To further understand the long-debated origin of the high-pressure cubic-rhombohedral transition in FeO, we investigated the domain wall structure in  $\text{Fe}_{0.94}\text{O}$  using high-pressure microdiffraction imaging techniques. The results reveal a non-reflection type domain wall structure forming due to the cubic-rhombohedral transition in  $\text{Fe}_{0.94}\text{O}$ , which suggests the transformation could be associated with defects and is unlikely to be ferroelastic in nature. © 2012 American Institute of Physics. [doi:10.1063/1.3679117]

Stoichiometric ferrous oxide FeO does not exist at ambient conditions, and its formula is more accurately represented by  $\text{Fe}_{1-x}\text{O}$ , with the deviation from stoichiometry,  $x$ , ranging from 0.05 to 0.15. This non-stoichiometry is associated with defect clusters consisting of octahedral cation vacancies and tetrahedral interstitial ferric  $\text{Fe}^{3+}$  cations.<sup>1</sup> At ambient conditions,  $\text{Fe}_{1-x}\text{O}$  is paramagnetic and adopts a cubic NaCl-type structure with these defect clusters. Upon compression,  $\text{Fe}_{1-x}\text{O}$  undergoes a series of phase transitions from cubic to rhombohedral then to NiAs-structures.<sup>2,3</sup> The first transition occurs at 10-16 GPa, as three of the four body diagonals of the cubic unit cell compress more than the fourth, leading to a rhombohedral distortion.<sup>2</sup> Since such a cubic-rhombohedral distortion could occur along any of the four energetically equivalent cubic body diagonal directions. The transition is consistent with the defining characteristics of a ferroic transition, in which the order parameter (such as electric polarization in ferroelectrics, magnetization in ferromagnets, or spontaneous strain in ferroelastics) has multiple energetically equivalent orientations (Fig. 1).<sup>4</sup>

It has been argued that the cubic-rhombohedral distortion is either ferroelastic<sup>5</sup> or antiferromagnetic in origin.<sup>2,6,7</sup> Growing evidence from experiments<sup>8-11</sup> and first-principles theory<sup>12</sup> has largely ruled out the possibility of an antiferromagnetic transition, but it is still unclear whether the cubic-rhombohedral transition is ferroelastic, ferroelectric, or multiferroic in character. Because ferroic transitions often lead to the formation of domains and the configurations of the domain walls are closely related to point group symmetry changes and to the nature of the transitions,<sup>4</sup> we developed a high-pressure technique by integrating the diamond-anvil cell with a nanoscale x-ray diffraction contrast imaging probe to study domain walls<sup>13</sup> forming in  $\text{Fe}_{0.94}\text{O}$ . The

unprecedented spatial resolution has enabled us to discover the formation of a non-reflection domain wall during the cubic-rhombohedral transition. This discovery suggests the transition could be associated with defects and is unlikely to be ferroelastic in origin but rather is possibly ferroelectric in nature.

$\text{Fe}_{0.94}\text{O}$  (with lattice parameter  $a = 4.308 \text{ \AA}$ ) was synthesized by procedures described before.<sup>14</sup> A  $40 \times 40 \times 15 \mu\text{m}^3$  single crystal was loaded with ruby as a pressure calibrant and helium as the pressure medium in a symmetric diamond anvil cell.<sup>5</sup> The surface normal of the sample was nearly parallel to the [001] zone axis of the sample, and the principle axes of the crystal were aligned so that they were nearly parallel to the axes of the sample scanning stages. The diffraction geometry in this experiment was similar to the zone-axis diffraction measurements on  $\text{Fe}_{1-x}\text{O}$  performed by Ding *et al.*<sup>15</sup> High pressure diffraction imaging measurements were performed on  $\text{Fe}_{0.94}\text{O}$  at high pressure in Sector 2-ID-D of the advanced photon source (APS), Argonne National Laboratory (ANL). An 18 keV x-ray beam was focused to  $\sim 300 \text{ nm}$  at the sample position.<sup>16</sup> The diffraction intensity at a selected

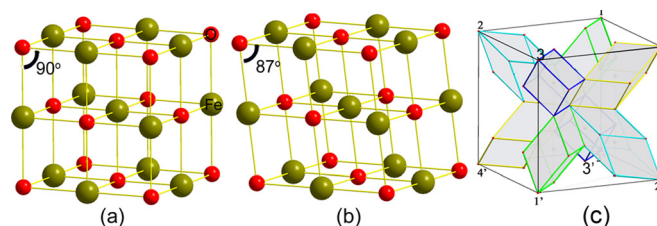


FIG. 1. (Color online) The structure models of  $\text{Fe}_{1-x}\text{O}$  at (a) ambient condition, which is NaCl-type cubic structure, (b) at 20 GPa, which is a rhombohedral structure. (c) The eight energetically equivalent variants in a cubic cell along the  $\langle 111 \rangle$  body diagonals that could be associated with the ferroic transition from cubic to rhombohedral symmetry.

<sup>a)</sup>Electronic mail: yangding@aps.anl.gov.

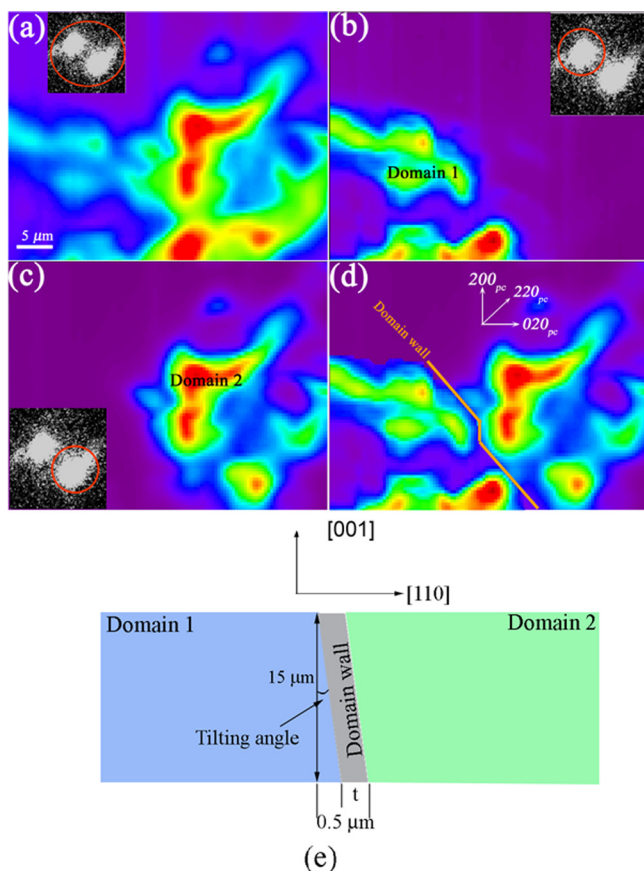


FIG. 2. (Color online) Diffraction intensity contrast maps for  $\text{Fe}_{0.94}\text{O}$  measured at 24.7 GPa. (a) A 2D diffraction map was obtained by including both of the split 220 peaks, as indicated by the red circle in the inset. (b),(c) Maps obtained by selecting only an individual peak (indicated by red circles in the insets). (d) Combination of maps in (b) and (c). The bold orange line represents the projected trace of the (110) domain wall. (e) The domain wall configuration viewed along  $[-110]$ . Based on the overlap and sample thickness, the wall tilting angle can be calculated as  $\arctan(0.5-t)/15$ , which is less than  $1.9^\circ$  (if  $t$  is not zero).

scattering vector (220 in this study) was recorded while the incident x-ray beam was rastered over the sample to obtain two-dimensional (2D) diffraction intensity maps.

The 2D diffraction intensity contrast imaging was measured at 7.5 and 24.7 GPa at 300 K. Diffraction patterns at 7.5 GPa show that the sample remained a single crystal, and no twinning domains were observed. At 24.7 GPa, the 220 reflection split into two peaks with different  $d$ -spacings (Fig. 2), while the 200 reflection persisted as a single peak, indicating that the cubic-rhombohedral transition had occurred within the sample. The average mosaicity of the reflection 220 at 7.5 GPa was measured as  $\sim 0.5^\circ$  and reached  $\sim 1.2^\circ$  at 24.7 GPa. This observation is consistent with previous single-crystal studies on  $\text{Fe}_{1-x}\text{O}$ .<sup>16,17</sup> In Figs. 2(b) and 2(c), intensity maps were obtained by selecting each of the split 220 peaks as imaging vectors. The results reveal that the peak splitting that occurs in the pressure-induced ferroic cubic-rhombohedral transition is associated with the formation of two domains. The measured lattice parameters for the first rhombohedral domain at regions close to the domain boundary are  $a = 2.9652(5)$  Å and  $\alpha = 57.75(3)^\circ$ ; for the second domain, they are  $a = 2.9633(7)$  Å and  $\alpha = 57.68(6)^\circ$ . In Fig. 3(a), the slight difference in the lattice parameters of the

two domains ( $\sim 0.06\%$ ) must have been caused by the strain of lattice planes induced by the mismatch between the two domains at the domain boundary.

As shown in Fig. 2, the domain wall that separates these two domains appears to be coherent. The spatial overlap of the two domains shown in Fig. 1(d) is less than  $0.5 \mu\text{m}$ ; thus, the wall is nearly vertical to the surface of the sample—i.e., the tilting angle of the domain wall is less than  $\arctan(0.5/15) = 1.9^\circ$  as shown in Fig. 2(e). The domain wall normal was determined to point in the [220] direction (for simplicity, cubic indexing is used), indicating a (110) domain wall. The intensity maps and their corresponding diffraction patterns, as well as the configuration of the two domains in 2D and 3D, are all illustrated in Fig. 3. From both the images and the diffraction patterns, it can be concluded that the (110) domain wall between two domains is not connected by a twin-like reflection plane, but rather by a 4-fold-like rotation axis along the [001] direction (Fig. 3). However, this non-reflection-type domain wall cannot be explained by ferroelastic transitions as previously speculated.

The cubic-rhombohedral transition has traditionally been treated as a second-order displacive transition occurring in the ideal NaCl-type structure with a symmetry of  $Fm\bar{3}m$ .<sup>3,5-7,12,18,19</sup> Since the symmetry of the rhombohedral phase has still not been determined definitively by experiment, it has been presumed to be  $\bar{R}3m$ , the highest centrosymmetric subgroup of  $Fm\bar{3}m$ .<sup>12,18,19</sup> As shown in Figs. 3(d) and 3(e), both group theory analysis and experiments<sup>20-22</sup> indicate that during a ferroelastic transition from  $m\bar{3}m$  to  $\bar{3}m$ , the resulting primary non- $180^\circ$  coherent domain walls from such transitions are reflection-type domain walls, namely, the mirror-like planes between two domains. The 4-fold rotation axis-related domain structure is only a secondary domain structure, which is a combination of a primary (100) reflection domain and a (110) reflection domain structure.<sup>20,21</sup> This secondary domain structure is in contrast to the primary non-reflection (110) domain structure observed in the  $\text{Fe}_{0.94}\text{O}$  in this study, and so far, this type of primary non-reflection (110) domain structure has only been observed in ferroelectric transitions.<sup>23</sup> Our result suggests that the transition in  $\text{Fe}_{0.94}\text{O}$  cannot be a ferroelastic transition, and the symmetry of the high-pressure phase has to be lower than  $\bar{3}m$ ,<sup>24</sup> i.e.,  $3m$ , a symmetry that is difficult to distinguish from  $\bar{3}m$  by experiment.

The occurrence of a high pressure phase with symmetry lower than  $\bar{3}m$  indicates that the defects must play a role in the structural stability of  $\text{Fe}_{1-x}\text{O}$  at high pressure since the rhombohedral distortion of a simple NaCl-type structure can only result in a  $\bar{3}m$  rhombohedral phase. Although the exact defect structures remain debated,<sup>1</sup> it is generally accepted that the defects tend to form larger clusters by stacking [4:1] defect clusters along three directions:  $\langle 100 \rangle$  (sharing faces),  $\langle 110 \rangle$  (sharing edges), or  $\langle 111 \rangle$  (sharing corners).<sup>25</sup> Moreover, recent theoretical calculations on wüstite predicted that  $\langle 111 \rangle$  stacking defect clusters are more stable than other configurations of clusters.<sup>25</sup> Therefore, the distortion from cubic to rhombohedral lattice could be associated with the  $\langle 111 \rangle$  defect clusters, and this is also possibly ferroelectric in nature. However, to obtain conclusive evidence for the ferroelectricity, it is necessary to demonstrate domain wall motion

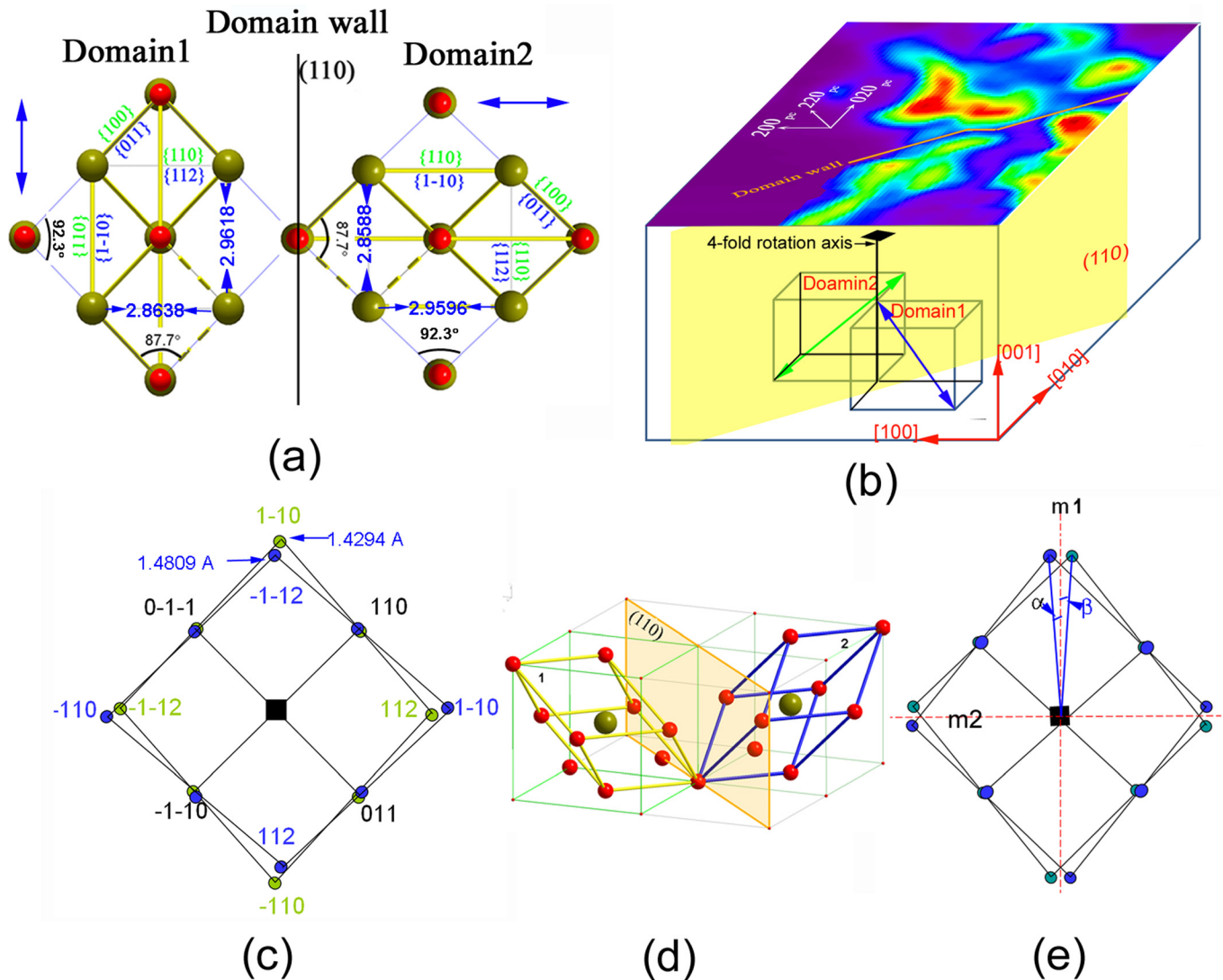


FIG. 3. (Color online) (a) Structure model and configuration of the rhombohedral domains in  $\text{Fe}_{0.94}\text{O}$ , viewed along the [001] direction; the indexing in green is based on a pseudocubic lattice, and the indexing in blue is based on a rhombohedral lattice. The blue arrows represent the elongation direction of the unit cells. (b) A 3D plot of the (110) domain wall in  $\text{Fe}_{0.94}\text{O}$  at 24.7 GPa; the blue and green arrows represent the longest body diagonals of the rhombohedral unit cells. The orientation of the two domains can be related by a 4-fold-like twin symmetry. (c) Simulated diffraction pattern corresponding to the rhombohedral domains of (a), viewed along the [001] axis; the indexing is based on the rhombohedral symmetry; the blue diffraction pattern corresponds to domain 1, and the green diffraction pattern corresponds to domain 2. The  $d$ -spacing of split reflections differs by 3.5%. (d) The model of the (110) reflection wall domains. (e) The corresponding simulated diffraction pattern of a reflection (110) wall domain viewed along the [001] axis; the blue diffraction pattern corresponds to domain 1, and the green diffraction pattern corresponds to domain 2. In the diffraction pattern, the  $m1$  and  $m2$  represent the mirror planes viewed along [001] direction. The  $d$ -spacing and angles ( $\alpha$  and  $\beta$ ) for the splitting 220 are identical.

under an applied electric field. This measurement could be achieved by applying a high DC field incrementally to the sample up to breakdown whilst imaging is accomplished. In addition, the hysteresis loops could be measured so as to extract spontaneous polarization and coercive field data to provide a domain scale evidence.

This research was supported by EFree, an Energy Frontier Research Center funded by the U.S. Department of Energy (DOE), Office of Science, Office of Basic Energy Sciences (BES) under Award Number DE-SC0001057. APS is supported by DOE-BES under Contract No. DE-AC02-06CH11357. Helium gas loading was performed at Sector 13, GSECARS (APS), which is supported by the NSF (EAR-0622171) and DOE (DE-FG02-94ER14466). This project is also supported by NSF (EAR 0911492) and CDAC: DOE/

NNSA (CDAC) (DE-FC52-08NA28554). H.W. Sheng is supported by ONR (N00014-09-1-1025A). W. L. Mao is supported by NSF (EAR-1141929).

<sup>1</sup>F. Koch and J. B. Cohen, *Acta Crystallogr. B* **25**, 275 (1969).

<sup>2</sup>T. Yagi, T. Suzuki, and S. Akimoto, *J. Geophys. Res.* **90**, 8784 (1985).

<sup>3</sup>Y. Fei and H.-K. Mao, *Science* **266**, 1678 (1994).

<sup>4</sup>V. K. Wadhawan, *Introduction to Ferroic Materials* (Gordon and Breach Science, Amsterdam, 2000).

<sup>5</sup>H.-K. Mao, J. Shu, Y. Fei, J. Hu, and R. J. Hemley, *Phys. Earth Planet. Inter.* **96**, 135 (1996).

<sup>6</sup>J. Badro, V. V. Struzhkin, J. Shu, R. J. Hemley, and H.-K. Mao, *Phys. Rev. Lett.* **83**, 4101 (1999).

<sup>7</sup>V. V. Struzhkin, H.-K. Mao, J. Hu, M. Schwoerer-Böhning, J. Shu, R. J. Hemley, W. Sturhahn, M. Y. Hu, E. E. Alp, P. Eng, and G. Shen, *Phys. Rev. Lett.* **87**, 255501 (2001).

<sup>8</sup>Y. Ding, J. Xu, C. T. Prewitt, R. J. Hemley, H.-K. Mao, J. A. Cowan, J. Zhang, J. Qian, S. V. Vogel, K. Lokshin, and Y. Zhao, *Appl. Phys. Lett.* **86**, 052505 (2005).

- <sup>9</sup>Y. Ding, Y. Ren, P. Chow, J. Zhang, S. V. Vogel, B. Winkler, J. Xu, Y. Zhao, and H.-K. Mao, *Phys. Rev. B* **74**, 144101 (2006).
- <sup>10</sup>I. Kantor, L. Dubrovinsky, C. McCammon, A. Kantor, S. Pascarelli, G. Aquilanti, W. Crichton, M. Mattesini, R. Ahuja, J. Almeida, and V. Urusov, *Phys. Chem. Miner.* **33**, 35 (2006).
- <sup>11</sup>A. P. Kantor, S. D. Jacobsen, I. Yu. Kantor, L. S. Dubrovinsky, C. A. McCammon, H. J. Reichmann, and I. N. Goncharenko, *Phys. Rev. Lett.* **93**, 215502 (2004).
- <sup>12</sup>D. G. Isaak, R. E. Cohen, M. J. Mehl, and D. J. Singh, *Phys. Rev. B* **47**, 7720 (1993).
- <sup>13</sup>P. G. Evans, E. D. Isaacs, G. Aeppli, Z. Cai, and B. Lai, *Science* **295**, 1042 (2002).
- <sup>14</sup>C. A. McCammon, C. A. Liu, and L.-G. Liu, *Phys. Chem. Miner.* **10**, 106 (1984).
- <sup>15</sup>Y. Ding, H. Liu, M. Somayazulu, Y. Meng, J. Xu, C. T. Prewitt, R. J. Hemley, and H.-K. Mao, *Phys. Rev. B* **72**, 174109 (2005).
- <sup>16</sup>J. Libera, Z. Cai, B. Lai, and S. Xu, *Rev. Sci. Instrum.* **73**, 1506 (2002).
- <sup>17</sup>J. Shu, H.-K. Mao, J. Hu, Y. Fei, and R. J. Hemley, *Neues Jahrb. Mineral., Abh.* **172**, 309 (1998).
- <sup>18</sup>R. E. Cohen, I. I. Mazin, and D. G. Isaak, *Science* **275**, 654 (1997).
- <sup>19</sup>W. L. Mao, J. Shu, J. Hu, R. J. Hemley, and H.-K. Mao, *J. Phys.: Condens. Matter.* **14**, 11349 (2002).
- <sup>20</sup>L. Wu and Y. Zhu, *Philos. Mag. A* **76**, 481 (1997).
- <sup>21</sup>W.-L. Wang, "Phase-transformation-induced twins in lanthanum gallate perovskite (LaGaO<sub>3</sub>)," Ph.D. dissertation (National Sun Yat-Sen University, 2006).
- <sup>22</sup>N. Orlovskaya, N. Browning, and A. Nicholls, *Acta Mater.* **51**, 5063 (2003).
- <sup>23</sup>J. Seidel, L. W. Martin, Q. He, Q. Zhan, Y.-H. Chu, A. Rother, M. E. Hawkrigde, P. Maksymovych, P. Yu, M. Gajek, N. Balke, S. V. Kalinin, S. Gemming, F. Wang, G. Catalan, J. F. Scott, N. A. Spaldin, J. Orenstein, and R. Ramesh, *Nat. Mater.* **8**, 229 (2009).
- <sup>24</sup>K. Aizu, *Phys. Rev. B* **2**, 754 (1970).
- <sup>25</sup>L. Minervini and R. W. Grimes, *J. Phys. Chem. Solid* **60**, 235 (1999).